Author Manuscript

Author Manuscript

Author Manuscript

Author Manuscript

HHS Public Access

Author manuscript

J Cell Physiol. Author manuscript; available in PMC 2024 July 16.

Published in final edited form as:

J Cell Physiol. 2014 April ; 229(4): 502–511. doi:10.1002/jcp.24470.

RGS2 Regulates Urotensin II-Induced Intracellular Ca^{2+} Elevation and Contraction in Glomerular Mesangial Cells

ADEBOWALE ADEBIYI*

Department of Physiology, University of Tennessee Health Science Center, Memphis, Tennessee

Abstract

Urotensin II (UII), a vasoactive peptide modulates renal hemodynamics. However, the physiological functions of UII in glomerular cells are unclear. In particular, whether UII alters mesangial tone remains largely unknown. The present study investigates the physiological effects of UII on glomerular mesangial cells (GMCs). This study also tested the hypothesis that the regulator of G-protein signaling (RGS) controls UII receptor (UTR) activity in GMCs. RT-PCR, Western immunoblotting, and immunofluorescence revealed UTR expression in cultured murine GMCs. Mouse UII (mUII) stimulated Ca^{2+} release from intracellular stores and activated store-operated Ca^{2+} entry (SOCE) in the cells. mUII also caused a reduction in planar GMC surface area. mUII-induced $[Ca^{2+}]_i$ elevation and contraction were attenuated by SB 657510, a UTR antagonist, araguspongin B, an inositol 1,4,5-trisphosphate receptor antagonist, thapsigargin, a sarco/endoplasmic reticulum Ca^{2+}-ATPase inhibitor, and La^{3+}, a store-operated Ca^{2+} channel blocker, but not nimodipine, an L-type Ca^{2+} channel blocker. In situ proximity ligation assay indicated molecular proximity between endogenous RGS2 and UTR in the cells. Treatment of GMCs with mUII elevated plasma membrane expression of RGS2 by ~2-fold. mUII also increased the interaction between RGS2 and UTR in the cells. siRNA-mediated knockdown of RGS2 in murine GMCs increased mUII-induced $[Ca^{2+}]_i$ elevation and contraction by ~35 and 31%, respectively. These findings indicate that mUII-induced SOCE results in murine GMC contraction. These data also suggest that UTR activation stimulates RGS2 recruitment to GMC plasma membrane as a negative feedback mechanism to regulate UTR signaling.

Glomerular mesangial cells (GMCs) are part of the morphofunctional units of the renal glomerulus (Latta, 1992). Apart from providing structural support for the glomerular capillaries, GMCs generate vasoactive mediators, growth factors, and cytokines (Schlondorff, 1987; Schlondorff and Banas, 2009). GMCs also express a variety of ion channels, including small, intermediate and large conductance Ca^{2+}-activated K^+ channels, Ca^{2+}-activated Cl, L-type Ca^{2+}, and receptor and store-operated Ca^{2+} channels (Stockand and Sansom, 1998; Ma et al., 2005). Vasoactive peptides, including angiotensin II (AngII), endothelin-1, and arginine vasopressin stimulate GMC contraction, whereas atrial natriuretic peptide, calcitonin gene-related peptide, and somatostatin cause GMC relaxation (Kurtz et al., 1989; Singhal et al., 1989; Garcia-Escribano et al., 1993; Diez-Marques et al., 1995;

*Correspondence to: Adebowale Adebiyi, Department of Physiology, College of Medicine, University of Tennessee Health Science Center, 894 Union Avenue, Memphis, TN 38163. aadebiyi@uthsc.edu.

Conflict of interest: Nothing to declare.

Author Manuscript Author Manuscript Author Manuscript Author Manuscript

Stockand and Sansom, 1997). GMC contraction and relaxation have been proposed to regulate glomerular filtration by altering glomerular capillary expansion and surface area (Iversen et al., 1992; Blantz et al., 1993; Stockand and Sansom, 1997).

Urotensin II (UII), a vasoactive peptide originally isolated from the fish has been characterized in several mammalian species, including mouse, rat, pig, monkey, and human (Pearson et al., 1980; Douglas et al., 2004). Whereas UII N-terminus is structurally variable, its C-terminus is conserved between species and required for its biological activities (Itoh et al., 1987; Conlon et al., 1990; Coulouarn et al., 1998; Douglas et al., 2004; Ross et al., 2010). Experimental evidence suggests that UII regulates renal functions, including renal blood flow (RBF), glomerular filtration rate (GFR), and electrolyte homeostasis. Infusion of human UII (hUII) into rat kidneys resulted in diuresis, natriuresis and an elevation in RBF and GFR (Zhang et al., 2003). Conversely, intravenous administration of rat UII attenuated urine flow, sodium and potassium excretion, RBF, and GFR in rats (Song et al., 2006; Abdel-Razik et al., 2008a,b). Intrarenal arterial injection of hUII also decreased RBF and renal cortical blood perfusion in neonatal pigs (Soni and Adebiyi, 2013). Immunoreactive UII has been localized to the integral components of the renal glomerulus, including the glomerular basement membrane, capillary endothelial cells, and mesangium (Shenouda et al., 2002; Balat et al., 2007). However, the physiological functions of UII in renal glomerular cells are unclear. In particular, it remains largely unknown whether UII alters mesangial tone. UTR, a G-protein-coupled receptor (GPCR) previously designated as an orphan receptor GPR14, mediates the physiological functions of UII (Ames et al., 1999; Liu et al., 1999; Mori et al., 1999; Nothacker et al., 1999; Elshourbagy et al., 2002). UTR is heterogeneously distributed in the kidney (Song et al., 2006; Abdel-Razik et al., 2008b). Mechanisms that regulate UTR signaling are unclear, but likely involve modulators of GPCR activity, including the regulator of G-protein signaling (RGS) (Douglas et al., 2000).

Agonist-induced activation of GPCRs is deactivated by rapid hydrolysis of bound GTP to GDP by the GTPase activity of the G_{α} subunit (Wettschureck and Offermanns, 2005). The intrinsic GTPase activity of G proteins is stimulated by RGS proteins (Ross and Wilkie, 2000; Hollinger and Hepler, 2002; Wettschureck and Offermanns, 2005). Over 20 multifunctional RGS proteins have been identified (Ross and Wilkie, 2000; Hollinger and Hepler, 2002). RGS proteins such as RGS2, RGS4, and RGS5 modulate G-protein signaling pathways associated with cardiovascular and renal functions, including AngII, adrenergic, muscarinic, mineralocorticoid, and vasopressin receptor-mediated signal transduction in blood vessels, heart, adrenal glands, and kidneys (Gu et al., 2009). Some RGS proteins, including RGS2, RGS4, RGS6, RGS7, RGS9, RGS11, and RGS19 selectively regulate G protein targets (Heximer et al., 1997, 1999; Ross and Wilkie, 2000; Hollinger and Hepler, 2002; Xie and Palmer, 2007). RGS2 selectively regulates $G_{\alpha q}$ functions, including inositol 1,4,5-trisphosphate (IP_3) production (Heximer et al., 1997, 1999; Kimple et al., 2009). UTR is coupled to $G_q/_{11}$ proteins and stimulated phosphoinositide hydrolysis in rabbit thoracic aorta upon activation by UII (Saetrum et al., 2000; Maguire and Davenport, 2002). Taken together, these studies suggest the possibility that RGS2 may regulate UTR functions.

In the present study, the physiological effects of UII-induced UTR activation in GMCs were investigated. This study also tested the hypothesis that endogenous RGS2 regulates UTR

Author Manuscript Author Manuscript Author Manuscript Author Manuscript

activity in GMCs. Findings here indicate that mouse UII (mUII) induces store-operated Ca^{2+} entry (SOCE) and contraction in murine GMCs. Data also suggest that mUII stimulates RGS2 recruitment to GMC plasma membrane as a negative feedback mechanism to regulate UTR activation.

Materials and Methods

Animals

Use of animals in this study was reviewed and approved by the Animal Care and Use Committee of the University of Tennessee Health Science Center (UTHSC). Mice (C57BL/6J) of 4–6 weeks age were purchased from the Jackson Laboratories (Bar Harbor, ME) and maintained at the UTHSC animal core facility.

GMC culture

A mouse GMC line was purchased from the American Type Culture Collection (Manassas, VA). Cells were subcultured in Dulbecco's modified Eagle's medium (DMEM; Life Technologies, Grand Island, NY) supplemented with mesangial cell growth medium (ScienCell Research Laboratories Carlsbad, CA), 2% fetal bovine serum (Atlanta Biologicals, Lawrenceville, GA), and 1% penicillin/streptomycin (Sigma-Aldrich, St. Louis, MO). Cultured GMCs were characterized by negative immunostaining for cytokeratin 18 (CYK18), an epithelial cell marker and positive staining for alpha smooth muscle actin (α-SMA), a myogenic marker (Mene et al., 1989; Supplemental Fig. 1).

Reverse transcription polymerase chain reaction (RT-PCR)

Total RNA was purified from mouse kidneys and cultured GMCs using the RNA MicroPrep kit (Zymo Research Corp., Orange, CA). cDNAs were synthesized from the RNA samples using the QuantiTect RT Kit (Qiagen, Valencia, CA) and were amplified by PCR using gene-specific oligonucleotide primer pairs (Table 1). PCR amplification was performed using the Eppendorf Mastercycler (Eppendorf, Westbury, NY) with the following reaction conditions: an initial denaturation at 98°C for 2 min, followed by 35 cycles (denaturation at 98°C for 10 sec, annealing at 57°C for 30 sec, and extension at 72°C for 30 sec), with a final extension at 72°C for 10 min. PCR products were resolved on 1.5% agarose gels stained with GelRed dye (Biotium, Hayward, CA) and documented on Kodak In Vivo F Pro Imaging System (Carestream Molecular Imaging, Rochester, NY). To confirm amplicons by sequencing analysis, PCR products were purified with ExoSAP-IT reagent (Affymetrix, Cleveland, OH). Thereafter, sequencing reactions were performed at the UTHSC Molecular Resource Center using the ABI 3130XL Genetic Analyzer (Applied Biosystems, Foster City, CA).

Western immunoblotting

Cultured GMCs were lyzed in ice-cold RIPA buffer (Thermo Scientific, Rockford, IL) followed by centrifugation to remove cell debris. Protein concentrations were determined using a Bio-Rad protein assay kit and SmartSpec 3000 Spectrophotometer (Bio-Rad, Hercules, CA). Protein lysates were mixed with SDS sample buffer containing 5% β-mercaptoethanol and boiled at ~95°C for 5 min. Proteins were then separated on 4–15%

Author Manuscript Author Manuscript Author Manuscript Author Manuscript

gradient polyacrylamide gels using the Mini Trans-Blot Cell (Bio-Rad) and transferred onto polyvinylidene difluoride or nitrocellulose membranes using a Semi-Dry Blotter (Thermo Scientific). Nonspecific binding sites on the membranes were blocked by BupH Tris Buffered Saline (Thermo Scientific) supplemented with 0.1% Tween 20 (TBS-T) and 5% nonfat milk for 1 h at room temperature. The membranes were probed with respective primary antibodies overnight at 4°C. After extensive wash in TBS-T, the membranes were incubated in horseradish peroxidase-conjugated secondary antibodies for 1 h at room temperature and washed in TBS-T. Immunoreactive proteins were visualized on a Kodak Imaging system using a Pierce Chemiluminescence kit (Thermo Scientific). For quantification, protein band intensities were normalized to those of GAPDH and analyzed by digital densitometry using Quantity One software (Bio-Rad).

Biotinylation of cell surface proteins

Sub-confluent GMCs were washed with ice-cold phosphate buffered saline (PBS) and incubated with 1 mg/ml of EZ-Link Sulfo-NHS-LC-Biotin (Thermo Scientific) for ~45 min at 4°C. Afterward, the cells were washed with PBS and incubated with 100 mM glycine in ice-cold PBS for 30 min at 4°C to remove unbound biotin. The cells were then lyzed in RIPA buffer (Thermo Scientific) followed by spectrophotometric determination of protein concentration. Dynabeads streptavidin (40 μL; Life Technologies) were mixed with the protein and incubated at 4°C with gentle rotation for 1 h. A DynaMag magnet (Life Technologies) was used to separate proteins bound to Dynabeads streptavidin from supernatant containing non-biotinylated cytosolic proteins. The beads were washed six times in PBS containing 0.1% BSA. Immobilized biotinylated proteins were eluted from Dynabeads by boiling the samples for 5 min in SDS buffer containing 5% β-mercaptoethanol. Proteins were then resolved using Western immunoblotting.

Immunofluorescence staining and confocal microscopy

GMCs grown on glass coverslips were fixed in 4% formaldehyde for 20 min and permeabilized with 0.2% Triton X-100 for 20 min at room temperature. After 1 h of incubation in PBS containing 5% BSA to block non-specific binding sites, cells were treated overnight at 4°C with respective antibodies (1:40, each). Next day, cells were washed with PBS and incubated with DyLight 488-conjugated pre-adsorbed anti-rabbit or DyLight 550-conjugated pre-adsorbed anti-mouse secondary antibodies (1:50, each) for 1 h at room temperature. Following wash and mount, images were acquired with a Zeiss LSM Pascal laser-scanning confocal microscope. DyLight 488 and DyLight 550 were excited at 488 and 543 nm and emission collected at 505–530 and >560 nm, respectively. Colocalization was determined using Coloc_2 analysis tool in Fiji image processing software (Schindelin et al., 2012). Mander's overlap coefficient was used to quantify the degree of colocalization following background subtraction.

In situ proximity ligation assay (PLA)

Endogenous UTR and RGS2 interaction in GMCs was studied using the Duolink in situ PLA kit (Olink Bioscience, Uppsala, Sweden) (Soderberg et al., 2006). GMCs were cultured sparsely in a 16-well glass chamber slide (Thermo Scientific). The cells were fixed and permeabilized using immunofluorescence staining protocol described above. After blocking

Author Manuscript Author Manuscript Author Manuscript Author Manuscript

nonspecific binding sites with Duolink blocking solution, GMCs were incubated with anti-UTR and anti-RGS2 antibodies (1:40, each) overnight at 4°C in Duolink antibody diluent. Negative control slides were incubated with anti-UTR only or anti-RGS2 plus anti-UTR pre-incubated with a UTR antigen-blocking peptide. Next day, the cells were washed and incubated with Duolink secondary antibodies conjugated with oligonucleotides (anti-mouse PLA probe Minus and anti-rabbit PLA probe Plus) in a pre-heated humidity chamber for 1 h at 37°C. Thereafter, the cells were incubated with a ligation solution for 30 min at 37°C. The oligonucleotides hybridize to the two PLA probes only if they are in close proximity (<40 nm separation), while a ligase joins the two hybridized oligonucleotides to form a closed circle. Ligation of the oligonucleotides was followed by a rolling-circle amplification reaction, resulting in a repeated sequence product. The amplification products were then detected by a fluorescently labeled complementary oligonucleotide detection probes. Slides were mounted with a mounting medium containing DAPI nuclear stain (Olink Bioscience). PLA signals (red fluorescent dots) were imaged and analyzed using Zeiss confocal microscope and Duolink Image Tool (Olink Bioscience), respectively.

siRNA transfection

Transfection complexes consisting of siRNA and siPORT NeoFX Transfection Reagent (Life Technologies) were prepared in Opti-MEM medium (Life Technologies). GMCs were transfected with a pool of 3 target-specific RGS2 siRNA (~1 μg) or a non-targeting control siRNA (Santa Cruz Biotechnology, Inc., Santa Cruz, CA) for 72 h. Effective knockdown of RGS2 was confirmed by Western immunoblotting.

Intracellular Ca^{2+} $[Ca^{2+}]_i$ imaging

GMCs were seeded sparsely on 29 mm glass-bottom dishes with 14 mm micro-well (In Vitro Scientific, Sunnyvale, CA). The cells were washed three times in PBS and incubated with Fura-2-acetoxymethyl ester (Fura-2 AM; 10 μM), and 0.5% pluronic F-127 for ~45 min at room temperature in modified Krebs' solution (MKS; 134 mM NaCl, 6 mM KCl, 1.2 mM $CaCl_2$, 1 mM $MgCl_2$, 10 mM HEPES, and 5.5 mM glucose, pH 7.4). The cells were then washed for ~30 min before imaging to de-esterify Fura-2 AM molecules. $[Ca^{2+}]_i$ imaging was performed at room temperature using a ratiometric fluorescence system (Ionoptix Corp., Milton, MA) coupled to a Zeiss Axio Observer A1 inverted microscope equipped with a Fluar 40× oil-immersion objective. Fura-2 fluorescence was recorded by exciting at wavelengths of 340 and 380 nm using a hyperswitch light source (Ionoptix Corp.). Fura-2 fluorescence was collected simultaneously from cells located in the same field. Only one field was imaged per dish. Background-subtracted Fura-2 ratios were collected at 510 nm using a MyoCam-S CCD digital camera (Ionoptix Corp.) and analyzed with IonWizard software (Ionoptix Corp.).

GMC contractility measurement

GMC contraction was measured at room temperature by recording changes in planar surface area of individual GMC plated in glass-bottom dishes. Digital images of cells with well-defined perimeters were documented. Cell perimeters under control and experimental conditions were outlined and planar surface area calculated using ImageJ software (NIH,

Author Manuscript Author Manuscript Author Manuscript Author Manuscript

Bethesda, MD). The surface area of a GMC after treatment with a pharmacological agent was compared with its original size.

Antibodies and chemicals

Mouse monoclonal anti-RGS2 and rabbit polyclonal anti-CYK18 antibodies were purchased from Abgent, Inc. (San Diego, CA). Rabbit polyclonal anti-UTR antibodies were purchased from Alpha Diagnostic International, Inc. (San Antonio, TX) and Alomone Lab (Jerusalem, Israel). Mouse monoclonal anti-GAPDH antibody was purchased from GeneScript (Piscataway, NJ). Anti-α-SMA primary and DyLight conjugated secondary antibodies were purchased from Abcam (Cambridge, MA). HRP-conjugated anti-rabbit and anti-mouse secondary antibodies were purchased from Thermo Scientific and Abcam, respectively. 2,3,6-tri-O-butyryl-myo-inositol 1,4,5-trisphosphate-hexakis (acetoxymethyl) ester (Bt-IP_3), Fura-2 AM, Pluronic F-127, mUII, SB657510, araguspongin B, thapsigargin, Lanthanum (III) chloride heptahydrate, nimodipine, glycine, and β-mercaptoethanol were purchased from A.G. Scientific (San Diego, CA), Life Technologies, AnaSpec (Fremont, CA), Phoenix Pharmaceuticals (Burlingame, CA), Tocris Bioscience (Bristol, UK), Cayman Chemical (Ann Arbor, MI), Axxora (San Diego, CA), Sigma-Aldrich, Tocris, MP Biomedical (Solon, OH), and Sigma-Aldrich, respectively.

Data analysis

All data are expressed as mean ± standard error of mean (SEM). Changes in peak Fura-2 340/380 nm emission ratio were determined. Statistical analysis was calculated using InStat statistics software (Graph Pad, Sacramento, CA). Statistical significance was determined using Student's *t*-tests for paired or unpaired data and analysis of variance with Student–Newman–Keuls post hoc test for multiple comparisons. A P value <0.05 was considered significant.

Results

UTR is expressed in murine GMCs

PCR amplification with primers specific for UTR generated an amplicon of the expected size (513 bp) from mouse kidney and GMC cDNAs (Fig. 1A). Western blot analysis using a polyclonal rabbit anti-UTR antibody (Alpha Diagnostic International) revealed a prominent ~45 kDa band, slightly higher than the expected 42 kDa (Fig. 1B). Another immunoreactive band of ~85 kDa was detected on the blots (Fig. 1B). These bands were blocked by preabsorption of the antibody with a UTR antigen-blocking peptide (Fig. 1B). Immunostaining and confocal microscopy also detected UTR in the cells (Fig. 1C). These data indicate that UTR is expressed in murine GMCs.

mUII elevates $[Ca^{2+}]_i$ in murine GMCs

The physiological function of UII in GMCs was investigated by exploring the effect of mUII on $[Ca^{2+}]_i$ in murine GMCs. mUII (1 μM) increased Fura-2 ratio from a baseline of 0.67 ± 0.03 to a peak of 1.62 ± 0.13 (n = 14), indicating that mUII elevates $[Ca^{2+}]_i$ concentration in GMCs. SB657510, a selective UTR antagonist did not alter basal $[Ca^{2+}]_i$ when applied alone (Supplemental Fig. 2A), but attenuated mUII-induced $[Ca^{2+}]_i$ elevation

Author Manuscript Author Manuscript Author Manuscript Author Manuscript

in the cells (Fig. 2A,B). Next, the role of inositol 1,4,5-trisphosphate receptor (IP_3R)-mediated endoplasmic reticulum (ER) Ca^{2+} release in mUII-induced $[Ca^{2+}]_i$ elevation was studied. Inhibition of ER-localized IP_3Rs by araguspongin B did not change basal $[Ca^{2+}]_i$ level when applied alone (Supplemental Fig. 2A), but attenuated $[Ca^{2+}]_i$ elevation induced by Bt-IP_3, a membrane permeant IP_3R agonist (Supplemental Fig. 2B,C). Araguspongin B also reduced mUII-induced $[Ca^{2+}]_i$ elevation in murine GMCs (Fig. 2B). These data suggest that IP_3R-mediated ER Ca^{2+} release contributes to mUII-induced $[Ca^{2+}]_i$ elevation in murine GMCs. Depletion of the ER Ca^{2+} store with thapsigargin, a sarco/endoplasmic reticulum Ca^{2+}-ATPase (SERCA) inhibitor increased Fura-2 ratio from a baseline of ~0.64 to a peak of ~1.6 (Supplemental Fig. 2A) and essentially abolished mUII-induced $[Ca^{2+}]_i$ elevation in murine GMCs (Fig. 2B). Nimodipine, an L-type Ca^{2+} channels blocker did not alter both basal and mUII-induced $[Ca^{2+}]_i$ elevation in murine GMCs (Fig. 2B and Supplemental Fig. 2A). La^{3+}, a store-operated Ca^{2+} (SOC) channel blocker did not change basal GMC $[Ca^{2+}]_i$ when applied alone (Supplemental Fig. 2A), but significantly reduced mUII-induced $[Ca^{2+}]_i$ elevation in the cells (Fig. 2B). In the absence of extracellular Ca^{2+}, mUII caused a transient increase in Fura-2 ratio indicative of Ca^{2+} release from the ER store (Fig. 2C,D). Subsequent addition of extracellular Ca^{2+} resulted in a larger increase in $[Ca^{2+}]_i$ (Fig. 2C,D). Collectively, these findings indicate that activation of UTR by mUII stimulates IP_3R-mediated ER Ca^{2+} release, leading to SOCE and an elevation in $[Ca^{2+}]_i$ concentration in murine GMCs.

mUII stimulates murine GMC contraction

The functional effect of mUII-induced $[Ca^{2+}]_i$ elevation in murine GMCs was studied by measuring changes in planar cell surface area. mUII caused a ~20% reduction in planar GMC surface area (Fig. 3A,B). Thapsigargin reduced GMC surface area by ~23% when applied alone (Supplemental Fig. 3). However, SB657510, araguspongin B, nimodipine, and La^{3+} did not significantly change original cell surface area (Supplemental Fig. 3). As shown in Figure 3B, mUII-induced decrease in planar GMC surface area was attenuated by SB657510, araguspongin B, thapsigargin, and La^{3+}. In contrast, mUII-induced reduction in cell surface area was unaltered by nimodipine (Fig. 3B). These data show that mUII-induced SOCE results in murine GMC contraction.

Endogenous RGS2 and UTR colocalize and interact in murine GMCs

Regulation of UTR by endogenous RGS2 was investigated. First, RGS2 expression in murine GMCs was examined. RT-PCR experiments revealed that RGS2 (amplicon size: 555 bp) is expressed in the cells (Fig. 4A). Western immunoblotting using a monoclonal mouse anti-RGS2 antibody also detected a ~24 kDa band, corresponding to the approximate molecular mass of RGS2 (Fig. 4B). Next, immunofluorescence staining and in situ PLA were used to investigate colocalization and interaction between endogenous UTR and RGS2 in murine GMCs. Confocal laser scanning microscopy showed that UTR colocalizes with RGS2 in the cells (Percentage of colocalization: 59.6 ± 1.4; n = 20 cells; Fig. 4C). PLA signals are detected when two PLA probes bind to two different antibodies that are bound to proteins in close proximity (illustrated in Fig. 4D). PLA signals (red fluorescent dots) were absent in control GMCs labeled with only anti-UTR antibody or anti-RGS2 plus anti-UTR pre-incubated with a UTR antigen-blocking peptide indicating that there is no

Author Manuscript Author Manuscript Author Manuscript Author Manuscript

non-specific binding of the PLA probes (Fig. 4D). In contrast, PLA signals were detected in GMCs labeled with anti-UTR and anti-RGS2 antibodies. Collectively, these data suggest that endogenous RGS2 and UTR colocalize and interact in murine GMCs.

mUII elevates plasma membrane RGS2 expression in murine GMCs

Figure 4C suggests that a portion of RGS2 is located intracellularly. To investigate whether activation of UTR recruits RGS2 to the plasma membrane, the cellular distribution of RGS2 and proximity between endogenous RGS2 and UTR in control and mUII-treated murine GMCs was studied using cell surface protein biotinylation and in situ PLA. GAPDH, an intracellular protein was detected in total and non-biotinylated, but not in biotinylated protein fractions (Fig. 5A,C). These results suggest that the biotinylated fractions contained only plasma membrane proteins. Treatment of murine GMCs with mUII did not alter RGS2 total protein (Fig. 5A,B). Approximately 6% of RGS2 total protein was present in biotinylated fractions of untreated GMCs (Fig. 5C,D). However, ~14% of RGS2 total protein was detected in biotinylated fraction of GMCs treated with mUII (Fig. 5C,D). Treatment of murine GMCs with mUII also elevated PLA signals in the cells by ~25% (Fig. 5E). These findings indicate that RGS2 is predominantly localized intracellularly in murine GMCs, and that activation of UTR by UII elevates the association between endogenous RGS2 and UTR in the cells.

RGS2 inhibits mUII-induced $[Ca^{2+}]_i$ elevation and contraction in murine GMCs

Transfection of GMCs with RGS2 siRNA reduced RGS2 protein expression by ~63% (Fig. 6A,B). However, RGS2 siRNA did not alter UTR protein expression (Fig. 6A,B). mUII-induced $[Ca^{2+}]_i$ elevation was increased by ~35% in RGS2 siRNA-transfected cells (Fig. 7A,B). Similarly, mUII-induced decrease in planar cell surface area was larger (~31%) in RGS2 siRNA-transfected cells when compared with the control (Fig. 7C). These data indicate that endogenous RGS2 inhibits mUII-induced $[Ca^{2+}]_i$ elevation and contraction in murine GMCs. Collectively, these findings suggest that mUII stimulates redistribution of RGS2 to GMC plasma membrane as a negative feedback mechanism to regulate mUII-induced $[Ca^{2+}]_i$ elevation and contraction (Fig. 8).

Discussion

The main findings of this study are that: (1) UTR is expressed in murine GMCs; (2) mUII stimulates $[Ca^{2+}]_i$ elevation and contraction in murine GMCs; (3) mUII-induced $[Ca^{2+}]_i$ elevation and contraction in murine GMCs are inhibited by SB 657510, a UTR antagonist, araguspongin B, an IP_3R antagonist, thapsigargin, a SERCA inhibitor, and La^{3+}, a SOC channel blocker, but not nimodipine, an L-type Ca^{2+} channel blocker; (4) endogenous RGS2 localizes with UTR in murine GMCs; (5) mUII elevates RGS2 plasma membrane association and interaction between RGS2 and UTR in murine GMCs; (6) siRNA-mediated knockdown of RGS2 increases mUII-induced $[Ca^{2+}]_i$ elevation and contraction in murine GMCs. In summary, this study provides new evidence indicating that UII modulates mesangial tone by stimulating SOCE, and that this physiological activity is regulated by RGS2.

Author Manuscript Author Manuscript Author Manuscript Author Manuscript

UTR expression has been demonstrated in rat renal arterioles, distal tubules, inner medullary collecting duct and thin limbs of Henlé and porcine renal epithelial cell line and afferent arterioles (Matsushita et al., 2003; Song et al., 2006; Soni and Adebiyi, 2013). Data from the present study signify that UTR is also expressed in renal GMCs. The molecular mass of UTR is ~42 kDa (Boucard et al., 2003). A ~60 kDa glycosylated form of UTR has also been observed in COS-7 cells overexpressing UTR, human adrenal samples, and newborn pig renal afferent arterioles (Boucard et al., 2003; Giuliani et al., 2009; Soni and Adebiyi, 2013). Here, immunoreactive bands migrating at ~45 and 85 kDa were essentially abolished by UTR antigen blocking peptide. Conceivably, the ~45 and 85 kDa bands represent unglycosylated and glycosylated UTR isoforms, respectively.

This study reveals for the first time that UII-induced activation of UTR stimulates $[Ca^{2+}]_i$ elevation and reduces planar GMC surface area, indicating that the physiological actions of UII in the kidney include regulation of mesangial tone. Genetic and structural similarities between UII and somatostatin peptides have been proposed (Pearson et al., 1980; Tostivint et al., 2006). UII also activated UTR and somatostatin receptors in rat aorta, CHO-K1 cells expressing porcine somatostatin receptors, and HEK293/aeq17 cells stably expressing rat UTR (Liu et al., 1999; Rossowski et al., 2002; Malagon et al., 2008). However, in contrast to the effect of UII observed in this study, somatostatin relaxed human GMCs (Garcia-Escribano et al., 1993; Diez-Marques et al., 1995). Thus, it appears that despite their structural similarities, UII and somatostatin differentially regulate GMC contraction. GMC contractility is controlled by different Ca^{2+} signaling pathways, including SOCE, receptor-operated Ca^{2+} entry (ROCE), and Ca^{2+} influx through L-type Ca^{2+} channels (Iijima et al., 1991; Stockand and Sansom, 1998; Du et al., 2007). SOCE activation occurs following depletion of SR/ER Ca^{2+} in response to activation of PLC-coupled GPCRs (Parekh and Putney, 2005). Conversely, ROCE activation is independent of SR/ER Ca^{2+} release (Parekh and Putney, 2005). Here, depletion of ER Ca^{2+} store essentially abolished mUII-induced $[Ca^{2+}]_i$ elevation in murine GMCs. ER Ca^{2+} depletion also attenuated mUII-induced GMC contraction. La^{3+}, a non-selective cation channel blocker effectively blocked SOC channels in human GMCs (Ma et al., 2000). In this study, La^{3+} inhibited mUII-induced $[Ca^{2+}]_i$ elevation and contraction in murine GMCs. In contrast, blockade of L-type Ca^{2+} channels did not alter mUII-induced $[Ca^{2+}]_i$ elevation and contraction in the cells, suggesting that mUII-induced $[Ca^{2+}]_i$ elevation and contraction in murine GMCs occur independently of L-type Ca^{2+} channels. Taken together, these data indicate that activation of UTR by UII stimulates SOCE and contraction in GMCs, consistent with a recent study in vascular smooth muscle cells (Dominguez-Rodriguez et al., 2012).

The molecular components of SOC channels have been described to include the transient receptor potential (TRP) and Orai channels and stromal interacting molecule 1 (STIM1), an ER-localized Ca^{2+} sensor (Salido et al., 2011). UII-induced SOCE in rat coronary artery smooth muscle cells and vasoconstriction are mediated by STIM1 and Orai1 channels (Dominguez-Rodriguez et al., 2012). Native SOC channels in human GMCs have been proposed to include the canonical transient receptor potential (TRPC) 1, 4, and STIM1 complexes (Sours-Brothers et al., 2009). A study has also demonstrated that TRPC4 channels mediate SOCE in murine GMCs (Wang et al., 2004). Perhaps, mUII-induced SOCE in murine GMCs involves STIM1 protein and Orai1, and/or TRPC channels.

Author Manuscript Author Manuscript Author Manuscript Author Manuscript

However, given the molecular and functional diversity of SOC channels in different cell types, future investigations are necessary to delineate the molecular components of SOC channels that mediate mUII-induced $[Ca^{2+}]_i$ elevation and contraction in murine GMCs.

Accumulating evidence suggests that renal RGS2 is involved in mechanisms that underlie cardiovascular homeostasis. Mice lacking RGS2 developed renal vascular hypertrophy and hypertension (Heximer et al., 2003). RGS2 regulates vasopressin-mediated renal water reabsorption capacity in mice (Zuber et al., 2007). Ablation of RGS2 from non-renal tissues, including peripheral blood vessels did not alter blood pressure in mice, whereas mice lacking RGS2 only in the kidneys developed hypertension, suggesting that direct renal actions of RGS2 regulate blood pressure (Gurley et al., 2010). Expressions of RGS3 and RGS5 have been demonstrated in adult and fetal mouse GMCs, respectively (Gruning et al., 1999; Cho et al., 2003). Overexpression of RGS3 in human GMCs reduced endothelin-1-induced $[Ca^{2+}]_i$ elevation and mitogen-activated protein kinase activity (Dulin et al., 1999). However, there is a paucity of information regarding the physiological functions of endogenous RGS proteins in GMCs. Findings here show for the first time that RGS2 is expressed in GMCs. Immunofluorescence staining indicated that endogenous RGS2 is localized in the plasma membrane, cytoplasmic, and nuclear regions of murine GMCs. These data are consistent with previous studies indicating that RGS2 protein is distributed between the plasma membrane and cytosolic cellular compartments (Bowman et al., 1998; Heximer et al., 2001; Salim et al., 2003; Gu et al., 2007; Takimoto et al., 2009). However, in another report, RGS2 was located in the nuclei, but not in the plasma membrane of COS-7 cells expressing GFP-tagged RGS2 (Chatterjee and Fisher, 2000). These conflicting findings suggest that cellular localization of RGS2 may be dependent on cell type. Additionally, cellular distribution of transiently expressed RGS2 in mammalian cells may inadequately reflect that of the endogenous protein. Molecular proximity between endogenous RGS2 and UTR in unstimulated GMCs suggests that a basal coupling may exist between the two proteins. It is also possible that some RGS2 proteins are associated with the plasma membrane and/or plasma membrane-localized proteins in close spatial proximity to UTR. Indeed, RGS2 exhibits a stable association with the plasma membrane of HEK cells via its N-terminal amphipathic domain (Heximer et al., 2001; Gu et al., 2007). RGS2 can also interact with and regulate ion channels at the plasma membrane independently of GPCR signaling (Schoeber et al., 2006). Cell surface protein biotinylation showed that a large portion of endogenous RGS2 is localized intracellularly. To test the hypothesis that UII-induced activation of UTR relocalizes RGS2 to the plasma membrane, the cellular distribution of RGS2 and proximity between endogenous RGS2 and UTR in mUII-treated GMCs were studied. Treatment of GMCs with UII did not alter RGS2 total protein. However, mUII elevated plasma membrane, but reduced cytosolic fractions of RGS2 protein. PLA also suggest that mUII increased the interaction between RGS2 and UTR in the cells. Hence, it appears that UII-induced activation of UTR recruits more RGS2 to the plasma membrane. Similarly, endothelin-1 stimulated RGS3 translocation from the cytosol to the plasma membrane in human GMCs stably overexpressing RGS3 (Dulin et al., 1999). In contrast, agonists did not alter plasma membrane localization of GFP-RGS2 in HEK293 cells overexpressing β_2 adrenergic, M_2 muscarinic, and AngII AT_{1A} receptors (Roy et al., 2003). It is possible that agonist-induced redistribution of intracellular RGS

Author Manuscript Author Manuscript Author Manuscript Author Manuscript

proteins is dependent on cell type and/or whether endogenous or overexpressed proteins are studied. mUII-induced RGS2 plasma membrane association may act as a negative feedback regulation of UTR activation in GMCs. The hypothesis that RGS2 regulates UTR signaling in murine GMCs is supported by data showing an increase in mUII-induced $[Ca^{2+}]_i$ elevation and contraction by targeted knockdown of RGS2.

In conclusion, the present study demonstrates that mUII-induced activation of UTR stimulates store-operated Ca^{2+} entry and contraction in murine GMCs. Findings here also suggest that UTR activation stimulates intracellular RGS2 recruitment to GMC plasma membrane as a negative feedback mechanism to regulate mUII-induced $[Ca^{2+}]_i$ elevation and contraction. Alterations in mesangial tone by vasoactive mediators may modulate renal filtration (Stockand and Sansom, 1997). Whether UII-induced contraction of GMCs alters glomerular hemodynamics requires further investigations.

Supplementary Material

Refer to Web version on PubMed Central for supplementary material.

Acknowledgements

Dr. Adebiyi is supported by grant HL096411 from the National Institute of Health.

Contract grant sponsor: National Institute of Health (USA); Contract grant number: HL096411.

Literature Cited

Abdel-Razik AE, Balment RJ, Ashton N. 2008a. Enhanced renal sensitivity of the spontaneously hypertensive rat to urotensin II. Am J Physiol Renal Physiol 295:F1239–F1247. [PubMed: 18701623]

Abdel-Razik AE, Forty EJ, Balment RJ, Ashton N. 2008b. Renal haemodynamic and tubular actions of urotensin II in the rat. J Endocrinol 198:617–624. [PubMed: 18577565]

Ames RS, Sarau HM, Chambers JK, Willette RN, Aiyar NV, Romanic AM, Louden CS, Foley JJ, Sauermelch CF, Coatney RW, Ao Z, Disa J, Holmes SD, Stadel JM, Martin JD, Liu WS, Glover GI, Wilson S, McNulty DE, Ellis CE, Elshourbagy NA, Shabon U, Trill JJ, Hay DW, Ohlstein EH, Bergsma DJ, Douglas SA. 1999. Human urotensin-II is a potent vasoconstrictor and agonist for the orphan receptor GPR14. Nature 401:282–286. [PubMed: 10499587]

Balat A, Karakok M, Yilmaz K, Kibar Y. 2007. Urotensin-II immunoreactivity in children with chronic glomerulonephritis. Ren Fail 29:573–578. [PubMed: 17654320]

Blantz RC, Gabbai FB, Tucker BJ, Yamamoto T, Wilson CB. 1993. Role of mesangial cell in glomerular response to volume and angiotensin II. Am J Physiol 264:F158–F165. [PubMed: 8430826]

Boucard AA, Sauve SS, Guillemette G, Escher E, Leduc R. 2003. Photolabelling the rat urotensin II/GPR14 receptor identifies a ligand-binding site in the fourth transmembrane domain. Biochem J 370:829–838. [PubMed: 12495432]

Bowman EP, Campbell JJ, Druey KM, Scheschonka A, Kehrl JH, Butcher EC. 1998. Regulation of chemotactic and proadhesive responses to chemoattractant receptors by RGS (regulator of G-protein signaling) family members. J Biol Chem 273:28040–28048. [PubMed: 9774420]

Chatterjee TK, Fisher RA. 2000. Cytoplasmic, nuclear, and golgi localization of RGS proteins. Evidence for N-terminal and RGS domain sequences as intracellular targeting motifs. J Biol Chem 275:24013–24021. [PubMed: 10791963]

Author Manuscript Author Manuscript Author Manuscript Author Manuscript

Cho H, Kozasa T, Bondjers C, Betsholtz C, Kehrl JH. 2003. Pericyte-specific expression of Rgs5: Implications for PDGF and EDG receptor signaling during vascular maturation. FASEB J 17:440–442. [PubMed: 12514120]

Conlon JM, Arnold-Reed D, Balment RJ. 1990. Post-translational processing of prepro-urotensin II. FEBS Lett 266:37–40. [PubMed: 2365069]

Coulouarn Y, Lihrmann I, Jegou S, Anouar Y, Tostivint H, Beauvillain JC, Conlon JM, Bern HA, Vaudry H. 1998. Cloning of the cDNA encoding the urotensin II precursor in frog and human reveals intense expression of the urotensin II gene in motoneurons of the spinal cord. Proc Natl Acad Sci USA 95:15803–15808. [PubMed: 9861051]

Diez-Marques ML, Garcia-Escribano C, Medina J, Boyano-Adanez MC, Arilla E, Torrecilla G, Rodriguez-Puyol D, Rodriguez-Puyol M. 1995. Effects of somatostatin on cultured human mesangial cells. Endocrinology 136:3444–3451. [PubMed: 7628380]

Dominguez-Rodriguez A, Diaz I, Rodriguez-Moyano M, Calderon-Sanchez E, Rosado JA, Ordonez A, Smani T. 2012. Urotensin-II signaling mechanism in rat coronary artery: Role of STIM1 and Orai1-dependent store operated calcium influx in vasoconstriction. Arterioscler Thromb Vasc Biol 32:1325–1332. [PubMed: 22223729]

Douglas SA, Sulpizio AC, Piercy V, Sarau HM, Ames RS, Aiyar NV, Ohlstein EH, Willette RN. 2000. Differential vasoconstrictor activity of human urotensin-II in vascular tissue isolated from the rat, mouse, dog, pig, marmoset and cynomolgus monkey. Br J Pharmacol 131:1262–1274. [PubMed: 11090097]

Douglas SA, Dhanak D, Johns DG. 2004. From ‘gills to pills’: Urotensin-II as a regulator of mammalian cardiorenal function. Trends Pharmacol Sci 25:76–85. [PubMed: 15102493]

Du J, Sours-Brothers S, Coleman R, Ding M, Graham S, Kong DH, Ma R. 2007. Canonical transient receptor potential 1 channel is involved in contractile function of glomerular mesangial cells. J Am Soc Nephrol 18:1437–1445. [PubMed: 17389736]

Dulin NO, Sorokin A, Reed E, Elliott S, Kehrl JH, Dunn MJ. 1999. RGS3 inhibits G protein-mediated signaling via translocation to the membrane and binding to Galpha11. Mol Cell Biol 19:714–723. [PubMed: 9858594]

Elshourbagy NA, Douglas SA, Shabon U, Harrison S, Duddy G, Sechler JL, Ao Z, Maleeff BE, Naselsky D, Disa J, Aiyar NV. 2002. Molecular and pharmacological characterization of genes encoding urotensin-II peptides and their cognate G-protein-coupled receptors from the mouse and monkey. Br J Pharmacol 136:9–22. [PubMed: 11976263]

Garcia-Escribano C, Diez-Marques ML, Gonzalez-Rubio M, Rodriguez-Puyol M, Rodriguez-Puyol D. 1993. Somatostatin antagonizes angiotensin II effects on mesangial cell contraction and glomerular filtration. Kidney Int 43:324–333. [PubMed: 8095076]

Giuliani L, Lenzini L, Antonello M, Aldighieri E, Belloni AS, Fassina A, Gomez-Sanchez C, Rossi GP. 2009. Expression and functional role of urotensin-II and its receptor in the adrenal cortex and medulla: Novel insights for the pathophysiology of primary aldosteronism. J Clin Endocrinol Metab 94:684–690. [PubMed: 19001524]

Gruning W, Arnould T, Jochimsen F, Sellin L, Ananth S, Kim E, Walz G. 1999. Modulation of renal tubular cell function by RGS3. Am J Physiol 276:F535–F543. [PubMed: 10198412]

Gu S, He J, Ho WT, Ramineni S, Thal DM, Natesh R, Tesmer JJ, Hepler JR, Heximer SP. 2007. Unique hydrophobic extension of the RGS2 amphipathic helix domain imparts increased plasma membrane binding and function relative to other RGS R4/B subfamily members. J Biol Chem 282:33064–33075. [PubMed: 17848575]

Gu S, Cifelli C, Wang S, Heximer SP. 2009. RGS proteins: Identifying new GAPs in the understanding of blood pressure regulation and cardiovascular function. Clin Sci (Lond) 116:391–399. [PubMed: 19175357]

Gurley SB, Griffiths RC, Mendelsohn ME, Karas RH, Coffman TM. 2010. Renal actions of RGS2 control blood pressure. J Am Soc Nephrol 21:1847–1851. [PubMed: 20847141]

Heximer SP, Watson N, Linder ME, Blumer KJ, Hepler JR. 1997. RGS2/G0S8 is a selective inhibitor of Gqalpha function. Proc Natl Acad Sci USA 94:14389–14393. [PubMed: 9405622]

Author Manuscript Author Manuscript Author Manuscript Author Manuscript

Heximer SP, Srinivasa SP, Bernstein LS, Bernard JL, Linder ME, Hepler JR, Blumer KJ. 1999. G protein selectivity is a determinant of RGS2 function. J Biol Chem 274:34253–34259. [PubMed: 10567399]

Heximer SP, Lim H, Bernard JL, Blumer KJ. 2001. Mechanisms governing subcellular localization and function of human RGS2. J Biol Chem 276:14195–14203. [PubMed: 11278586]

Heximer SP, Knutsen RH, Sun X, Kaltenbronn KM, Rhee MH, Peng N, Oliveira-dos-Santos A, Penninger JM, Muslin AJ, Steinberg TH, Wyss JM, Mecham RP, Blumer KJ. 2003. Hypertension and prolonged vasoconstrictor signaling in RGS2-deficient mice. J Clin Invest 111:445–452. [PubMed: 12588882]

Hollinger S, Hepler JR. 2002. Cellular regulation of RGS proteins: Modulators and integrators of G protein signaling. Pharmacol Rev 54:527–559. [PubMed: 12223533]

Iijima K, Moore LC, Goligorsky MS. 1991. Syncytial organization of cultured rat mesangial cells. Am J Physiol 260:F848–F855. [PubMed: 1711787]

Itoh H, Itoh Y, Rivier J, Lederis K. 1987. Contraction of major artery segments of rat by fish neuropeptide urotensin II. Am J Physiol 252:R361–R366. [PubMed: 3812773]

Iversen BM, Kvam FI, Matre K, Morkrid L, Horvei G, Bagchus W, Grond J, Ofstad J. 1992. Effect of mesangiolysis on autoregulation of renal blood flow and glomerular filtration rate in rats. Am J Physiol 262:F361–F366. [PubMed: 1348397]

Kimple AJ, Soundararajan M, Hutsell SQ, Roos AK, Urban DJ, Setola V, Temple BR, Roth BL, Knapp S, Willard FS, Siderovski DP. 2009. Structural determinants of G-protein alpha subunit selectivity by regulator of G-protein signaling 2 (RGS2). J Biol Chem 284:19402–19411. [PubMed: 19478087]

Kurtz A, Schurek HJ, Jelkmann W, Muff R, Lipp HP, Heckmann U, Eckardt KU, Scholz H, Fischer JA, Bauer C. 1989. Renal mesangium is a target for calcitonin gene-related peptide. Kidney Int 36:222–227. [PubMed: 2550694]

Latta H 1992. An approach to the structure and function of the glomerular mesangium. J Am Soc Nephrol 2:S65–S73. [PubMed: 1600139]

Liu Q, Pong SS, Zeng Z, Zhang Q, Howard AD, Williams DL Jr., Davidoff M, Wang R, Austin CP, McDonald TP, Bai C, George SR, Evans JF, Caskey CT. 1999. Identification of urotensin II as the endogenous ligand for the orphan G-protein-coupled receptor GPR14. Biochem Biophys Res Commun 266:174–178. [PubMed: 10581185]

Ma R, Smith S, Child A, Carmines PK, Sansom SC. 2000. Store-operated Ca^{2+} channels in human glomerular mesangial cells. Am J Physiol Renal Physiol 278:F954–F961. [PubMed: 10836983]

Ma R, Pluznick JL, Sansom SC. 2005. Ion channels in mesangial cells: Function, malfunction, or fiction. Physiology (Bethesda) 20:102–111. [PubMed: 15772299]

Maguire JJ, Davenport AP. 2002. Is urotensin-II the new endothelin? Br J Pharmacol 137:579–588. [PubMed: 12381671]

Malagon MM, Molina M, Gahete MD, Duran-Prado M, Martinez-Fuentes AJ, Alcain FJ, Tonon MC, Leprince J, Vaudry H, Castano JP, Vazquez-Martinez R. 2008. Urotensin II and urotensin II-related peptide activate somatostatin receptor subtypes 2 and 5. Peptides 29:711–720. [PubMed: 18289730]

Matsushita M, Shichiri M, Fukai N, Ozawa N, Yoshimoto T, Takasu N, Hirata Y. 2003. Urotensin II is an autocrine/paracrine growth factor for the porcine renal epithelial cell line, LLCPK1. Endocrinology 144:1825–1831. [PubMed: 12697688]

Mene P, Simonson MS, Dunn MJ. 1989. Physiology of the mesangial cell. Physiol Rev 69:1347–1424. [PubMed: 2678170]

Mori M, Sugo T, Abe M, Shimomura Y, Kurihara M, Kitada C, Kikuchi K, Shintani Y, Kurokawa T, Onda H, Nishimura O, Fujino M. 1999. Urotensin II is the endogenous ligand of a G-protein-coupled orphan receptor, SENR (GPR14). Biochem Biophys Res Commun 265:123–129. [PubMed: 10548501]

Nothacker HP, Wang Z, McNeill AM, Saito Y, Merten S, O'Dowd B, Duckles SP, Civelli O. 1999. Identification of the natural ligand of an orphan G-protein-coupled receptor involved in the regulation of vasoconstriction. Nat Cell Biol 1:383–385. [PubMed: 10559967]

Author Manuscript Author Manuscript Author Manuscript Author Manuscript

Parekh AB, Putney JW Jr. 2005. Store-operated calcium channels. Physiol Rev 85:757–810. [PubMed: 15788710]

Pearson D, Shively JE, Clark BR, Geschwind II, Barkley M, Nishioka RS, Bern HA. 1980. Urotensin II: A somatostatin-like peptide in the caudal neurosecretory system of fishes. Proc Natl Acad Sci USA 77:5021–5024. [PubMed: 6107911]

Ross EM, Wilkie TM. 2000. GTPase-activating proteins for heterotrimeric G proteins: Regulators of G protein signaling (RGS) and RGS-like proteins. Annu Rev Biochem 69:795–827. [PubMed: 10966476]

Ross B, McKendy K, Giaid A. 2010. Role of urotensin II in health and disease. Am J Physiol Regul Integr Comp Physiol 298:R1156–R1172. [PubMed: 20421634]

Rossowski WJ, Cheng BL, Taylor JE, Datta R, Coy DH. 2002. Human urotensin II-induced aorta ring contractions are mediated by protein kinase C, tyrosine kinases and Rho-kinase: Inhibition by somatostatin receptor antagonists. Eur J Pharmacol 438:159–170. [PubMed: 11909607]

Roy AA, Lemberg KE, Chidiac P. 2003. Recruitment of RGS2 and RGS4 to the plasma membrane by G proteins and receptors reflects functional interactions. Mol Pharmacol 64:587–593. [PubMed: 12920194]

Saetrum OO, Nothacker H, Ehlert FJ, Krause DN. 2000. Human urotensin II mediates vasoconstriction via an increase in inositol phosphates. Eur J Pharmacol 406:265–271. [PubMed: 11020490]

Salido GM, Jardin I, Rosado JA. 2011. The TRPC ion channels: Association with Orai1 and STIM1 proteins and participation in capacitative and non-capacitative calcium entry. Adv Exp Med Biol 704:413–433. [PubMed: 21290309]

Salim S, Sinnarajah S, Kehrl JH, Dessauer CW. 2003. Identification of RGS2 and type V adenylyl cyclase interaction sites. J Biol Chem 278:15842–15849. [PubMed: 12604604]

Schindelin J, Arganda-Carreras I, Frise E, Kaynig V, Longair M, Pietzsch T, Preibisch S, Rueden C, Saalfeld S, Schmid B, Tinevez JY, White DJ, Hartenstein V, Eliceiri K, Tomancak P, Cardona A. 2012. Fiji: An open-source platform for biological-image analysis. Nat Methods 9:676–682. [PubMed: 22743772]

Schlondorff D 1987. The glomerular mesangial cell: An expanding role for a specialized pericyte. FASEB J 1:272–281. [PubMed: 3308611]

Schlondorff D, Banas B. 2009. The mesangial cell revisited: No cell is an island. J Am Soc Nephrol 20:1179–1187. [PubMed: 19470685]

Schoeber JP, Topala CN, Wang X, Diepens RJ, Lambers TT, Hoenderop JG, Bindels RJ. 2006. RGS2 inhibits the epithelial Ca^{2+} channel TRPV6. J Biol Chem 281:29669–29674. [PubMed: 16895908]

Shenouda A, Douglas SA, Ohlstein EH, Giaid A. 2002. Localization of urotensin-II immunoreactivity in normal human kidneys and renal carcinoma. J Histochem Cytochem 50:885–889. [PubMed: 12070267]

Singhal PC, DeCandido S, Satriano JA, Schlondorff D, Hays RM. 1989. Atrial natriuretic peptide and nitroprusside cause relaxation of cultured rat mesangial cells. Am J Physiol 257:C86–C93. [PubMed: 2546436]

Soderberg O, Gullberg M, Jarvius M, Ridderstrale K, Leuchowius KJ, Jarvius J, Wester K, Hydbring P, Bahram F, Larsson LG, Landegren U. 2006. Direct observation of individual endogenous protein complexes in situ by proximity ligation. Nat Methods 3:995–1000. [PubMed: 17072308]

Song W, Abdel-Razik AE, Lu W, Ao Z, Johns DG, Douglas SA, Balment RJ, Ashton N. 2006. Urotensin II and renal function in the rat. Kidney Int 69:1360–1368. [PubMed: 16531985]

Soni H, Adebiyi A. 2013. Pressor and renal regional hemodynamic effects of urotensin II in neonatal pigs. J Endocrinol 217:317–326. [PubMed: 23554507]

Sours-Brothers S, Ding M, Graham S, Ma R. 2009. Interaction between TRPC1/TRPC4 assembly and STIM1 contributes to store-operated Ca^{2+} entry in mesangial cells. Exp Biol Med (Maywood) 234:673–682. [PubMed: 19307462]

Stockand JD, Sansom SC. 1997. Regulation of filtration rate by glomerular mesangial cells in health and diabetic renal disease. Am J Kidney Dis 29:971–981. [PubMed: 9186087]

Stockand JD, Sansom SC. 1998. Glomerular mesangial cells: Electrophysiology and regulation of contraction. Physiol Rev 78:723–744. [PubMed: 9674692]

Author Manuscript Author Manuscript Author Manuscript Author Manuscript

Takimoto E, Koitabashi N, Hsu S, Ketner EA, Zhang M, Nagayama T, Bedja D, Gabrielson KL, Blanton R, Siderovski DP, Mendelsohn ME, Kass DA. 2009. Regulator of G protein signaling 2 mediates cardiac compensation to pressure overload and antihypertrophic effects of PDE5 inhibition in mice. J Clin Invest 119:408–420. [PubMed: 19127022]

Tostivint H, Joly L, Lihrmann I, Parmentier C, Lebon A, Morisson M, Calas A, Ekker M, Vaudry H. 2006. Comparative genomics provides evidence for close evolutionary relationships between the urotensin II and somatostatin gene families. Proc Natl Acad Sci USA 103:2237–2242. [PubMed: 16467151]

Wang X, Pluznick JL, Wei P, Padanilam BJ, Sansom SC. 2004. TRPC4 forms store-operated Ca^{2+} channels in mouse mesangial cells. Am J Physiol Cell Physiol 287:C357–C364. [PubMed: 15044151]

Wettschureck N, Offermanns S. 2005. Mammalian G proteins and their cell type specific functions. Physiol Rev 85:1159–1204. [PubMed: 16183910]

Xie GX, Palmer PP. 2007. How regulators of G protein signaling achieve selective regulation. J Mol Biol 366:349–365. [PubMed: 17173929]

Zhang AY, Chen YF, Zhang DX, Yi FX, Qi J, Andrade-Gordon P, de GL, Li PL, Zou AP. 2003. Urotensin II is a nitric oxide-dependent vasodilator and natriuretic peptide in the rat kidney. Am J Physiol Renal Physiol 285:F792–F798. [PubMed: 12783779]

Zuber AM, Singer D, Penninger JM, Rossier BC, Firsov D. 2007. Increased renal responsiveness to vasopressin and enhanced V2 receptor signaling in $RGS2^{-/-}$ mice. J Am Soc Nephrol 18:1672–1678. [PubMed: 17475820]

Author Manuscript Author Manuscript Author Manuscript Author Manuscript

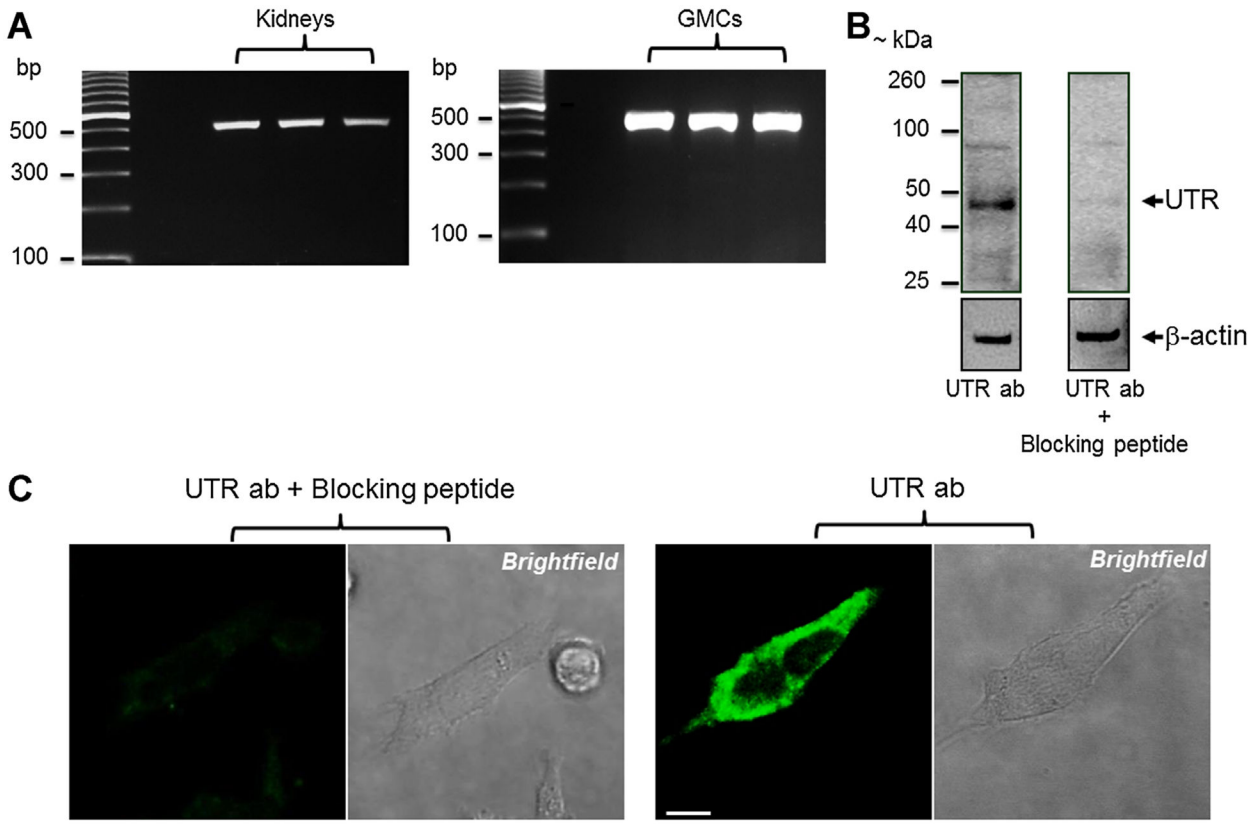

Fig. 1.

UTR is expressed in murine GMCs. A: Representative gel images showing PCR amplification of UTR transcript (513 bp) in murine kidneys and GMCs. Amplified UTR transcript was confirmed by sequencing analysis (data not shown). B: Western immunoblotting showing UTR protein isoforms in murine GMCs. Blots also show that a UTR antigen-blocking peptide blocks UTR detection. Blots were stripped and re-probed for β-actin. C: Immunofluorescence staining demonstrating UTR localization in murine GMCs. Negative controls prepared by preabsorption of UTR antibody with a UTR antigen-blocking peptide did not show fluorescence. Bar = 10 μm; ab, antibody.

Author Manuscript Author Manuscript Author Manuscript Author Manuscript

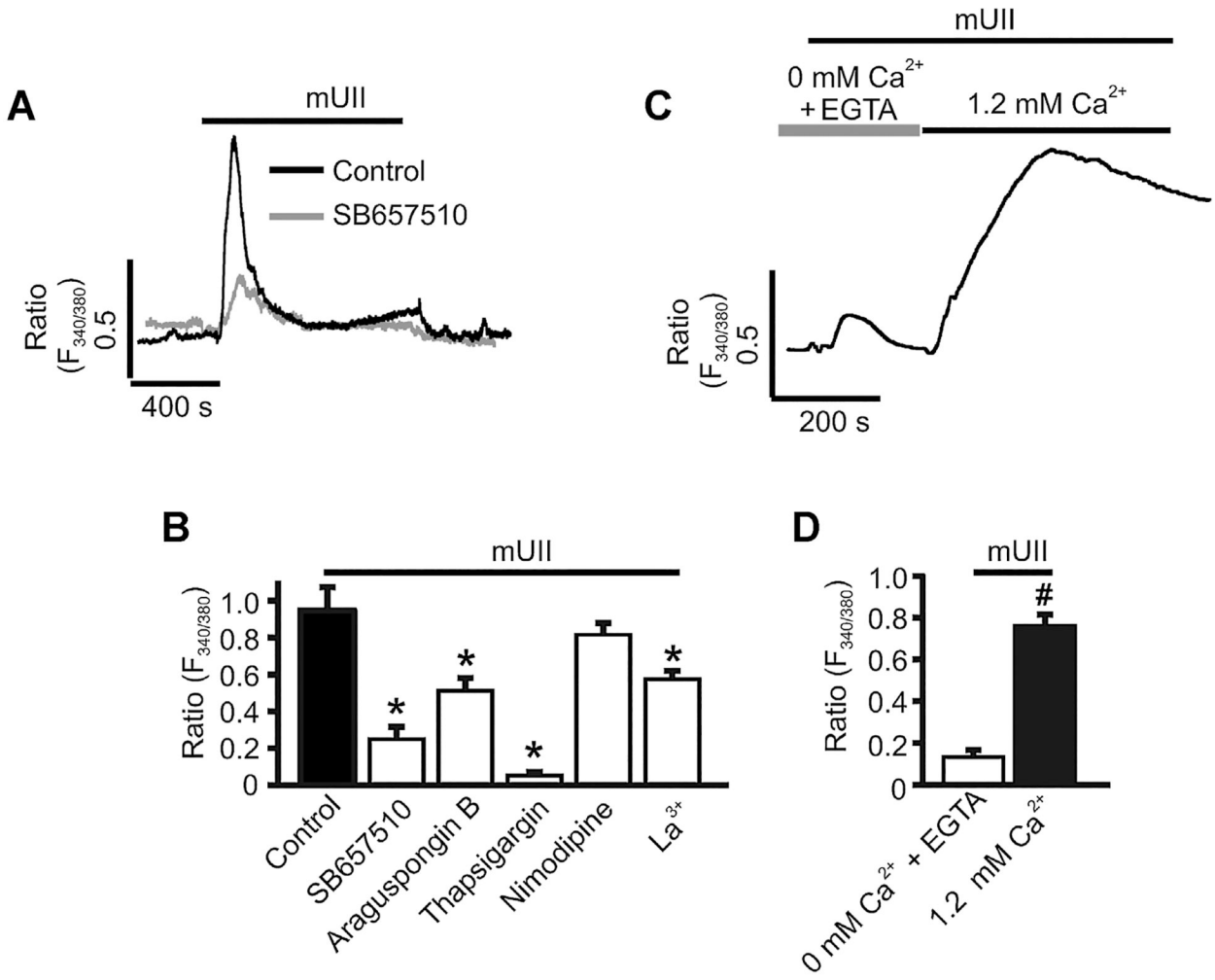

Fig. 2.

mUII elevates $[Ca^{2+}]_i$ in murine GMCs. A: Exemplar traces illustrating that mUII (1 μM)-induced $[Ca^{2+}]_i$ elevation is inhibited by SB657510 in murine GMCs. B: Mean mUII-induced changes in Fura-2 ratio in control (n = 14) and SB657510 (5 μM; n = 7)-, araguspongin B (3 μM; n = 6)-, thapsigargin (100 nM; n = 10)-, nimodipine (1 μM; n = 5)-, and La^{3+} (50 μM;n = 5)-treated murine GMCs. C: Exemplar trace illustrating mUII-induced SOCE in murine GMCs. D: Mean mUII-induced changes in Fura-2 ratio in the absence (+0.1 mM EGTA) and presence of extracellular Ca^{2+} (n = 8). Cells were pretreated with blockers/antagonists for ~15 min before the effects of mUII on $[Ca^{2+}]_i$ was measured. $^{*}P <$ 0.05 versus control; $^{\#}P < 0.05$ versus 0 mM Ca^{2+} +EGTA.

Author Manuscript Author Manuscript Author Manuscript Author Manuscript

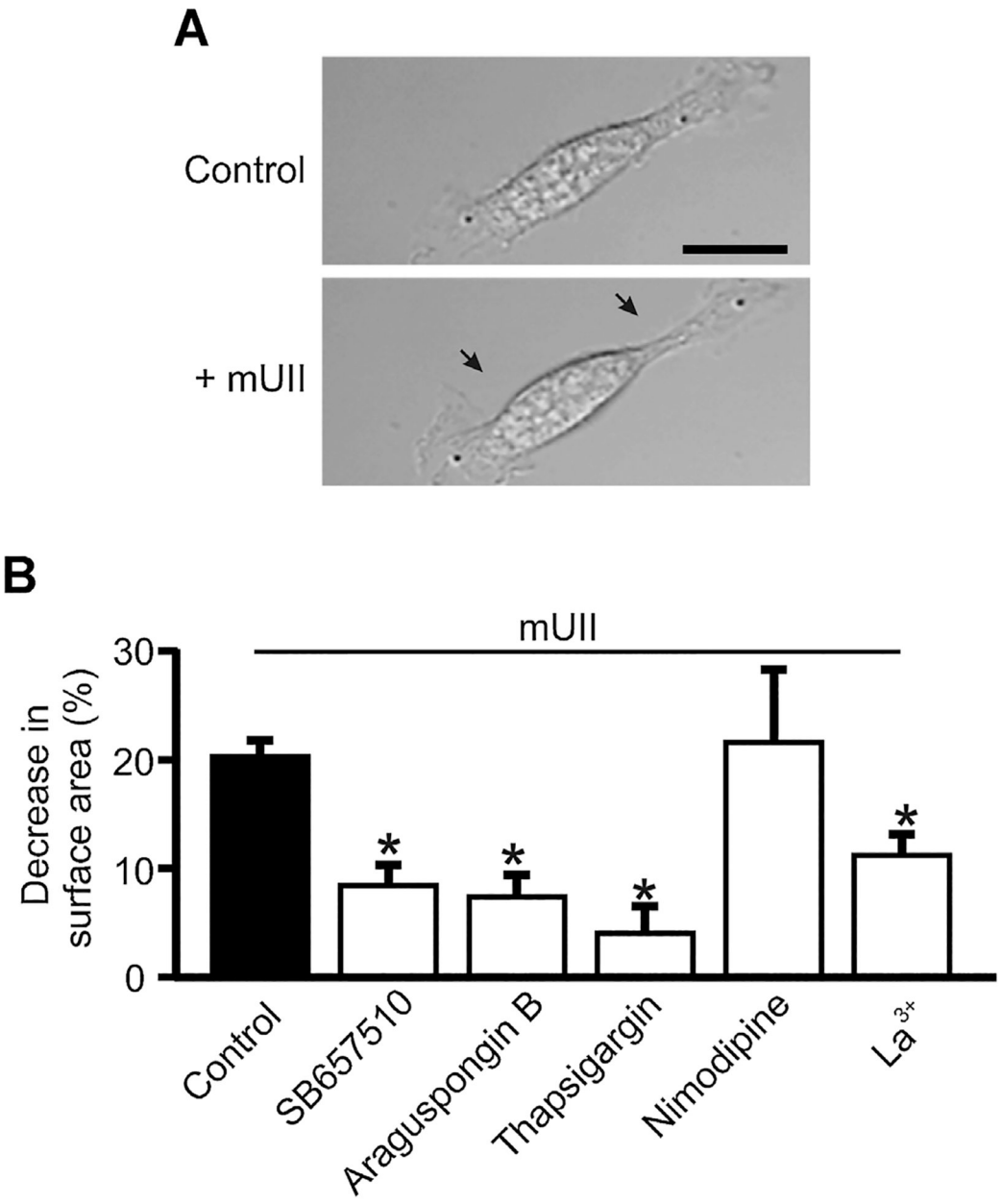

Fig. 3.

mUII stimulates murine GMC contraction. A: Original brightfield images showing a murine GMC before and after mUII (1 μM) treatment. Arrows indicate a reduction in planar cell surface area. B: Mean mUII-induced decrease in surface area in control (n = 15) and SB657510 (5 μM; n = 10)-, araguspongin B (3 μM;n = 10)-, thapsigargin (100 nM; n = 7)-, nimodipine (1 μM; n = 6)-, and La^{3+} (50 μM; n = 10)-treated murine GMCs. Cells were pretreated with blockers/antagonists for ~15 min before the effects of mUII on planar cell surface area was measured $*P < 0.05$ versus control. Bar = 20 μm.

Author Manuscript Author Manuscript Author Manuscript Author Manuscript

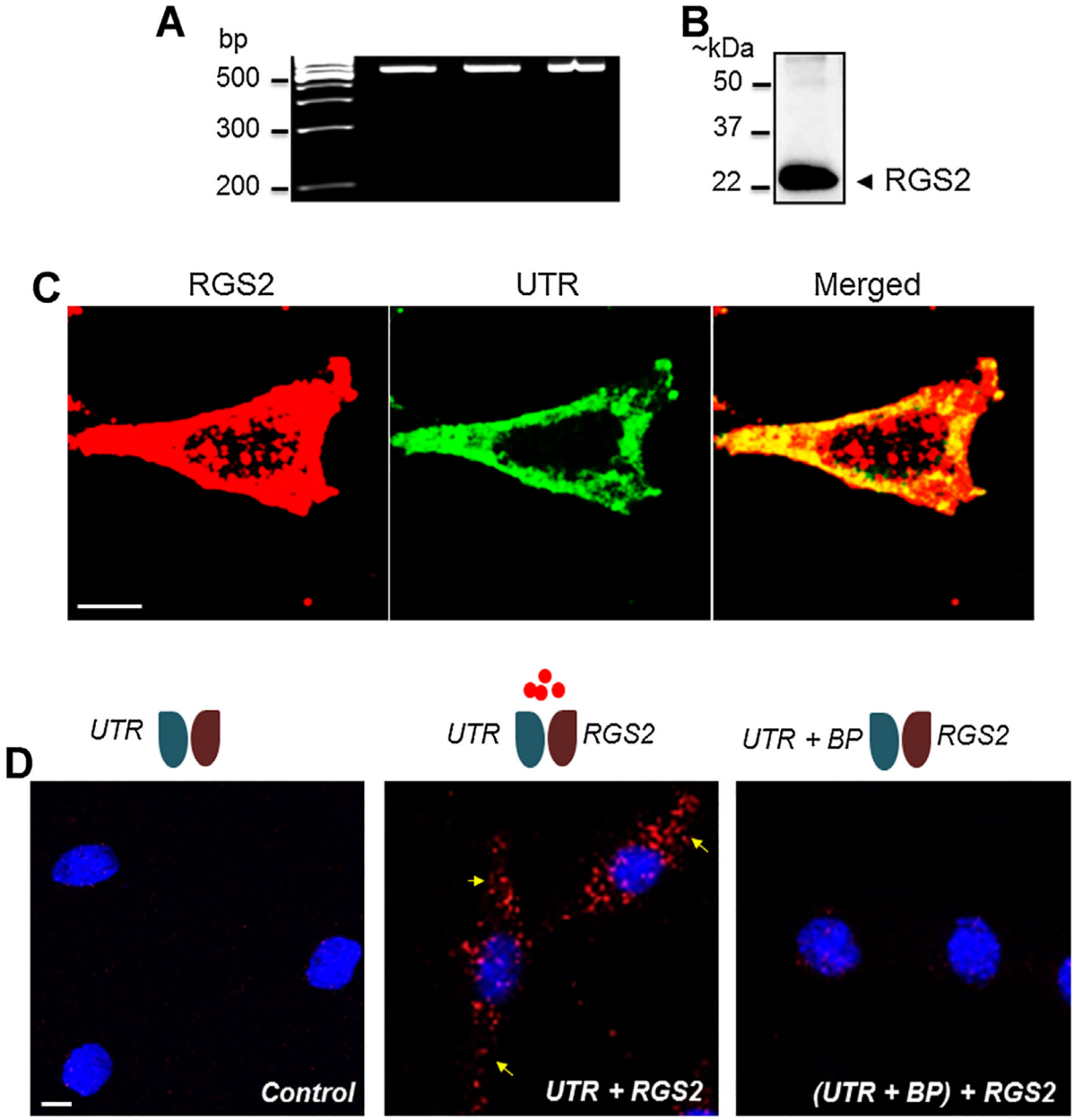

Fig. 4.

Endogenous RGS2 and UTR colocalize and interact in murine GMCs. A: A representative gel image showing RT-PCR amplification of RGS2 transcript (555 bp) in murine GMCs. Amplified RGS2 transcript was confirmed by sequencing analysis (data not shown). B: Western immunoblotting illustrating RGS2 protein expression in murine GMCs. C: Immunofluorescence staining of murine GMCs demonstrating that RGS2 colocalizes with UTR. D: In situ PLA detects interaction between UTR and RGS2 in murine GMCs. Yellow arrows point to PLA signals (red fluorescence). Illustrations on the panels indicate that PLA signals were absent in control cells labeled with only anti-UTR or anti-RGS2 plus anti-UTR pre-incubated with a UTR antigen-blocking peptide, whereas PLA signals were detected

in cells labeled with both anti-UTR and anti-RGS2 antibodies. Bar = 10 μm; BP, blocking peptide.

Author Manuscript Author Manuscript Author Manuscript Author Manuscript

Author Manuscript Author Manuscript Author Manuscript Author Manuscript

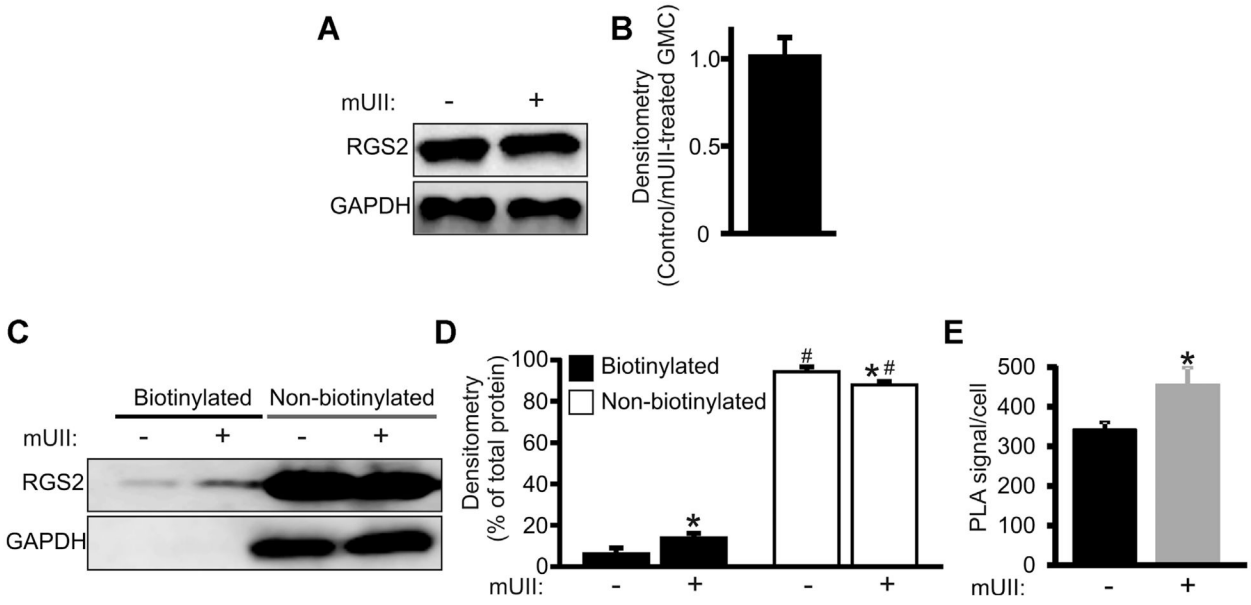

Fig. 5.

mUII elevates RGS2 plasma membrane association in murine GMCs. A: Western blot and (B) mean data (n = 4) illustrating that total endogenous RGS2 protein is unchanged in mUII (1 μM)-treated murine GMCs. C: Western blot and (D) mean data (n = 4 each) demonstrating that endogenous RGS2 is predominantly localized intracellularly in murine GMCs and that RGS2 plasma membrane expression is elevated in mUII-treated cells. Total and non-biotinylated immunoreactive protein bands were normalized to those of GAPDH. E: Mean data showing PLA signal per cell in control and mUII (1 μM)-treated murine GMCs. $^{\#}P < 0.05$ versus membrane RGS2; $^{*}P < 0.05$ versus untreated cells.

Author Manuscript Author Manuscript Author Manuscript Author Manuscript

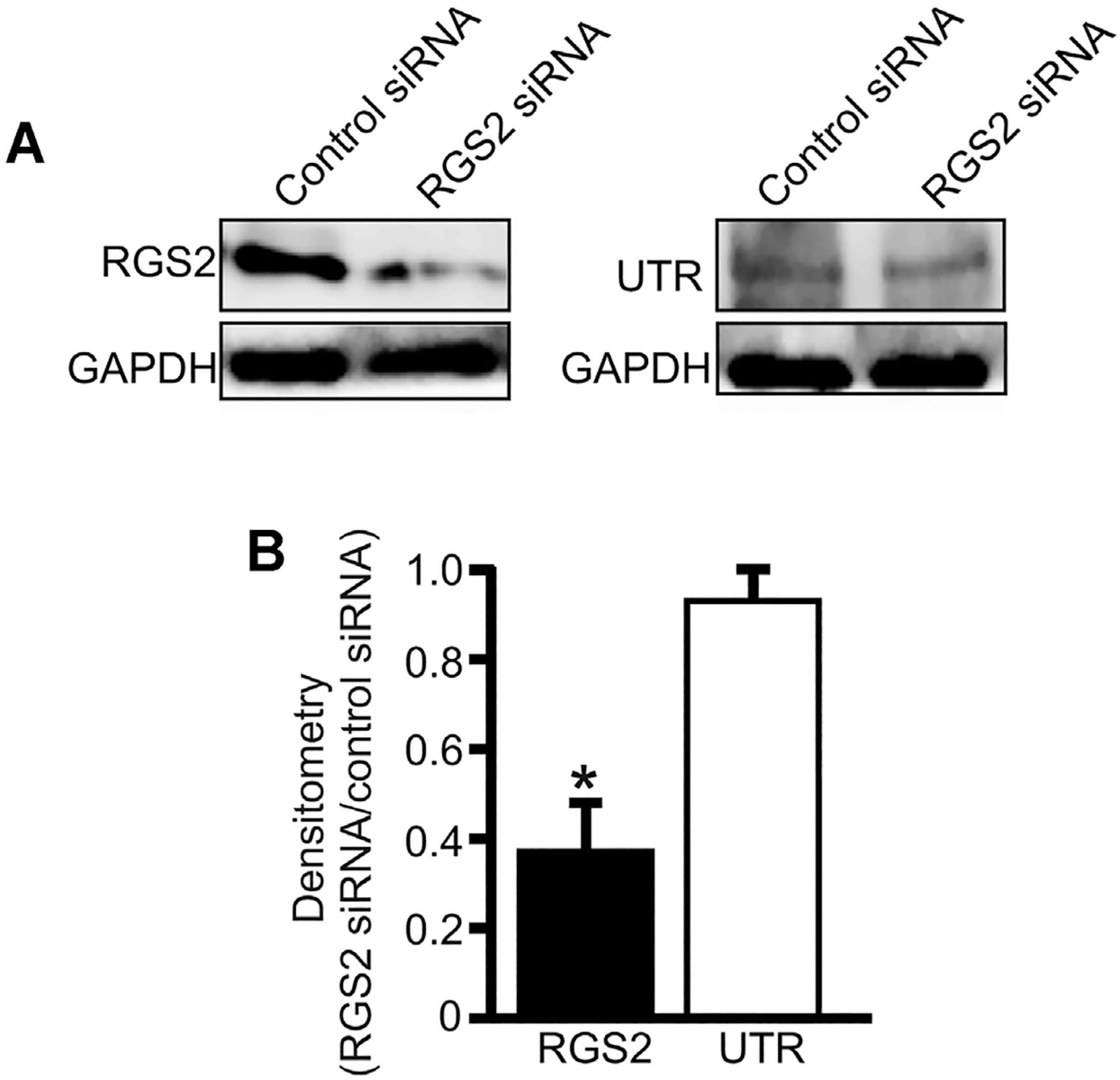

Fig. 6.

RGS2 knockdown does not alter UTR expression in murine GMCs. A: Western blot and (B) mean data (n = 5 each) illustrating that RGS2 siRNA induces knockdown of RGS2, but does not alter UTR protein expression in murine GMCs. $*P < 0.05$.

Author Manuscript Author Manuscript Author Manuscript Author Manuscript

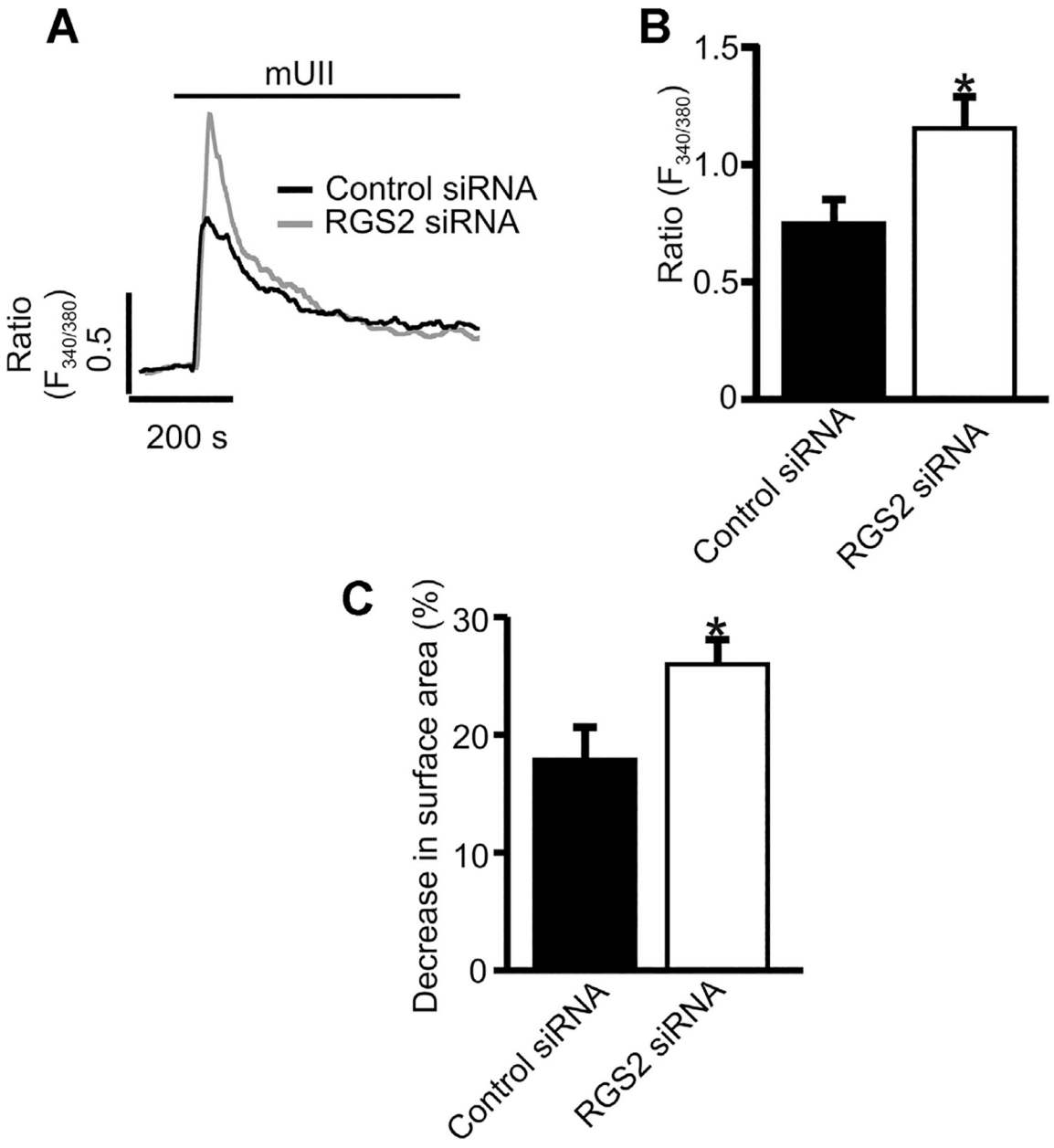

Fig. 7.

RGS2 inhibits mUII-induced $[Ca^{2+}]_i$ elevation and contraction in murine GMCs. A: Representative traces and (B) mean data illustrating mUII (1 μM)-induced changes in Fura-2 ratio in control siRNA (n = 9)- and RGS2 siRNA (n = 8)-transfected murine GMCs. C: Mean data showing mUII-induced reductions in surface area in control siRNA (n = 11)- and RGS2 siRNA (n = 12)-transfected murine GMCs. **P* < 0.05 versus control siRNA.

Author Manuscript Author Manuscript Author Manuscript Author Manuscript

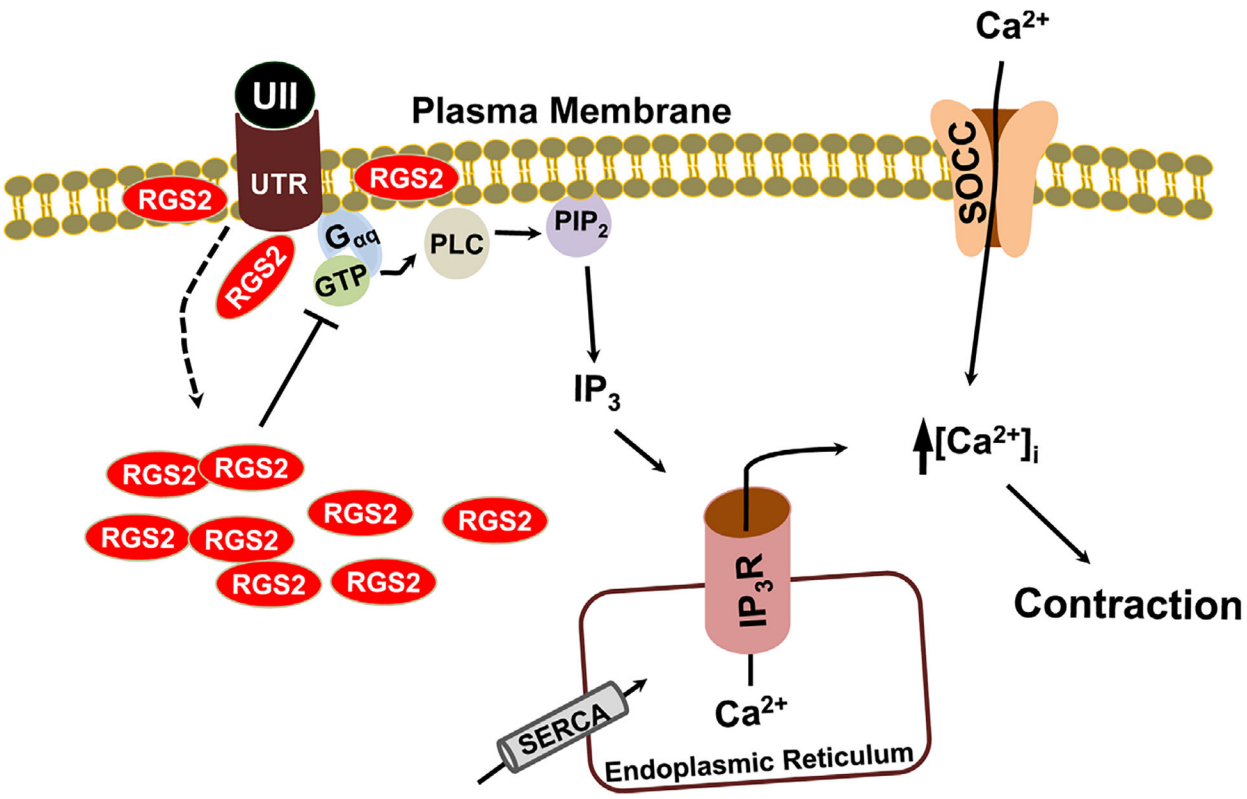

Fig. 8.

Schematic diagram of the hypothetical pathways by which RGS2 regulates UII-induced UTR activation in murine GMCs. UII-induced activation of $G_{\alpha q}$/11-coupled UTR stimulates PLC/IP_3-mediated ER Ca^{2+} release, resulting in Ca^{2+} entry via store-operated Ca^{2+} channels (SOCC) and contraction. A portion of RGS2 is associated with GMC plasma membrane. UII-induced activation of UTR recruits more intracellular RGS2 to the plasma membrane as a negative feedback mechanism to regulate UTR signaling. SERCA, sarco/endoplasmic reticulum Ca^{2+}-ATPase.

Author Manuscript

Author Manuscript

Author Manuscript

Author Manuscript

TABLE 1.

Oligonucleotide primer sequences

Gene	Sequence	GenBank accession number	Length (bp)
UTR		NM_145440.1	513
Forward	5′-TGCCATCCGGCTGGTCCGTA-3′		
Reverse	5′-TGCTGGAGGTGGACACGGCT-3′		
RGS2		NM_009061.4	555
Forward	5′-GACCGAATGCTGTGCCGTGC-3′		
Reverse	5′-TGCCCATGCCAGGTGTCTGGA-3′		